Egyptian Journal of Aquatic Biology & Fisheries
Zoology Department, Faculty of Science,
Ain Shams University, Cairo, Egypt.
ISSN 1110 – 6131
Vol. 26(5): 361 – 384 (2022)
www.ejabf.journals.ekb.eg

Identification of productive miter squid fishing grounds using a generalized additive model in Indonesian Fisheries Management Area 711

Hadi Puspito [1,*], Muhammad Helmi [2,4], Bambang Yulianto [3], Yassein A. Osman [6], Hoang Nguyen[5]

[1] Master Program of Marine Science, Diponegoro University, Prof Soedarto, Indonesia
[2] Department of Oceanography, Diponegoro University, Prof SoedartoSemarang, Indonesia
[3] Department of Marine Science, Diponegoro University, Prof Soedarto, Semarang, Indonesia
[4] Center for Coastal Disaster Mitigation and Rehabilitation, Diponegoro University, Indonesia
[5] Fisheries and Marine Institute of Memorial University of Newfoundland, A1C 5R3, Canada
[6] National Institute of Oceanography and Fisheries, NIOF, Cairo, Egypt
[*]**Corresponding Author: puspitohadi@gmail.com**

ARTICLE INFO

Article History:
Received: July 9, 2022
Accepted: Aug. 27, 2022
Online: Sept. 29, 2022

Keywords:
Squid,
Cast net,
Catch rate,
Remote sensing,
Vessel monitoring system

ABSTRACT

This study aimed to evaluate the factors affecting the catch rate and predict the potential catch for the determination of productive fishing grounds for miter squid (*Uroteuthis chinensis*) in the Indonesian Fisheries Management Area 711 for 2020. A vessel monitoring system and landing data from 66 cast nets were used to investigate catch per unit effort. Depth, chlorophyll-a, and sea surface temperature from satellite imagery combined with the month and geographic location of fishing were evaluated for their effect on catch per unit effort using a general additive model. The best model output was employed to identify productive fishing grounds. The results revealed that the average monthly catch rate ranged from 89.43- 337.47kg h^{-1}, with the highest occurring in May. Three significant variables affected the catch rate: month, latitude, and sea surface temperature, with contributions of 42.6%, 33.6%, and 12.7%, respectively. The catch rate continued to rise from March to May and tended to increase at higher latitudes where sea surface temperatures ranged from 27.6- 29.5°C or 31.5- 32.2°C. Based on the monthly map of predicted potential catch, the most productive fishing grounds were located in the waters between the islands of Anambas, Natuna, and Tambelan. These findings can support marine spatial planning and squid resource management in IFMA 711.

INTRODUCTION

The squid is an increasingly significant commodity in the global seafood trade, with Asian countries contributing to about sixty percent of world squid landings in 2019 **(SFP, 2022)**. However, the squid has been under heavy fishing pressure due to overexploitation **(Fauziyah *et al*., 2020; Wang *et al*., 2021)**. High fishing pressures cause rapid declines in squid stocks and harm marine ecosystems **(Arkhipkin *et al*., 2015)**. In addition, squid resources are best managed by effort limitation, considering that squid resources are short-lived ecological opportunists with a lifespan of about 1year; their populations are unstable, and environmental conditions influence their recruitment variability

(Rodhouse, 2001). These have gained interest in the need for improved marine spatial planning and management to ensure the long-term use of squid resources. One approach to support this is to effectively use oceanographic data and geospatial fisheries information to comprehend the productivity of fishing grounds.

Remotely sensed oceanic variables and squid fishery data analyzed in a geographic information system environment have aided in understanding fundamental relationships between squid resources and their aquatic environment **(Solanki *et al.*, 2017)**. Satellite data provided an opportunity to identify the spatial and temporal variation of environmental parameters in squid habitats affecting their ecological life **(Alabia *et al.*, 2015)**. Understanding ecological functions and structures in squid life requires knowledge of the physical and biological processes that govern squid population, distribution, and productivity at different spatial and temporal scales. The population demographic of squid was affected by coastal current, distribution of marine primary productivity, and the variation of habitat conditions **(Wang *et al.*, 2021)**. In addition, **Islam *et al.* (2017)** reported that depth contour is an essential factor in structuring the distribution of squid. Furthermore, sea surface temperature and chlorophyll-a concentration positively affected the monthly variation of squid abundance **(Yu *et al.*, 2019)**.

Numerous statistical modeling in a geospatial environment has frequently been used to characterize and forecast fishery resources **(Valavanis *et al.*, 2008)**. A generalized additive model (GAM) **(Hastie & Tibshirani, 1986)** is a statistical model that combines the properties of a general linear model and an additive model. In this model, the relationship between the response and predictors was modified by smooth functions to model and discover the data's non-linearities. This change allows the GAM to be more flexible than generalized linear or additive models. GAM's ability to deal with highly non-linear relationships between a dependent variable and a set of independent variables made it ideal for describing biological and ecological linkages **(Mugo *et al.*, 2010)**. GAM is a solution that offers an objective ability to estimate species abundance based on general ecology over a wide geographical area **(Solanki *et al.*, 2017)**. Many studies have been conducted on various species and catch predictions using GAM, such as billfishes, swimming crabs, Indian mackerel, and yellowfin tuna **(Nurdin *et al.*, 2017; Lan *et al.*, 2017; Naimullah *et al.*, 2020; Crespo-Neto *et al.*, 2021)**. **Maina *et al.* (2016)** recommended an integrated approach using remotely sensed data on oceanographic parameters, fishery data, and powerful statistical tools such as GAM to identify fishing grounds.

Cast net fishery is the dominant fishing industry for catching squid in the Indonesian Fisheries Management Area (IFMA) 711 **(Suryanto *et al.*, 2021)**. A cast net (Jala jatuh berkapal in Indonesian) with electric luring lights is a falling gear in Indonesia, commonly installed on fleet sizing more than 30 gross tonnages and equipped with a vessel monitoring system (VMS) transmitter. The main catch of cast net fishing, the miter squid (MS) *Uroteuthis chinensis*, is the focus of the present study. The MS, as a

positively phototactic species can be found at depths of up to 700 meters and exhibits morphological traits such as a slender and elongated mantle with a rhombic fin structure **(Jereb & Roper, 2010; Wulandari, 2018)**.

This study enhanced the merits of VMS, satellite-based data from cast net vessels for identifying fishing efforts and corresponding with landing data using geospatial techniques for characterizing MS catch rate variability in the IFMA 711. It then used a statistical approach based on GAM to assess the catch rate response to temporal, spatial, and marine environmental changes. For the application, satellite remote sensing data was used for oceanographic parameters, viz. bathymetry, sea surface chlorophyll-a, and sea surface temperature. Finally, the output data from the best model was used to determine productive fishing grounds. As a result, the current study aimed to evaluate the factors affecting the catch rate and map the potential catch.

MATERIALS AND METHODS

2.1. Study area

The study area focused on IFMA 711, with coordinates 102.29-111.05 °E and 4.13 °S to 7.79 °N, covering approximately 656,880 km2 (Fig. 1). IFMA 711 is located in northwest Indonesian waters, encompassing the Karimata Strait in the south, the Natuna Sea in the middle, and the South China Sea in the north **(MMAF, 2014)**. These are the fishing grounds for the cast net vessels that land the squid at the Tanjung Balai Karimun port.

2.2. Fishery data

The fishery data were collected from the Technical Executive Unit of Surveillance for Marine and Fisheries Resources based in Batam for 2020, which included MS landings recorded at the Tanjung Balai Karimun port and daily tracking VMS of vessel activities. MS is the main catch of cast net fishing along with its bycatches such as yellow stripe scad (*Selaroides leptolepis*), Indian mackerel (*Rastrelliger kanagurta*), and moonfish (*Mene maculata*). In this study, only MS catches were used as primary data. According to the fish landing data available for analysis, the data period (2020) was chosen as the last year with a complete 1-hour (interval) VMS record. The research used data from 66 cast net vessels ranging in size from 32 to 99 gross tonnages equipped with transmitter VMS, with a total fishing trip of 113. The vessels departed for the fishing grounds from February to June, then landed the catch at the port from March to the last day of November. The daily tracking VMS of all vessels showed as many as 418,453 point records.

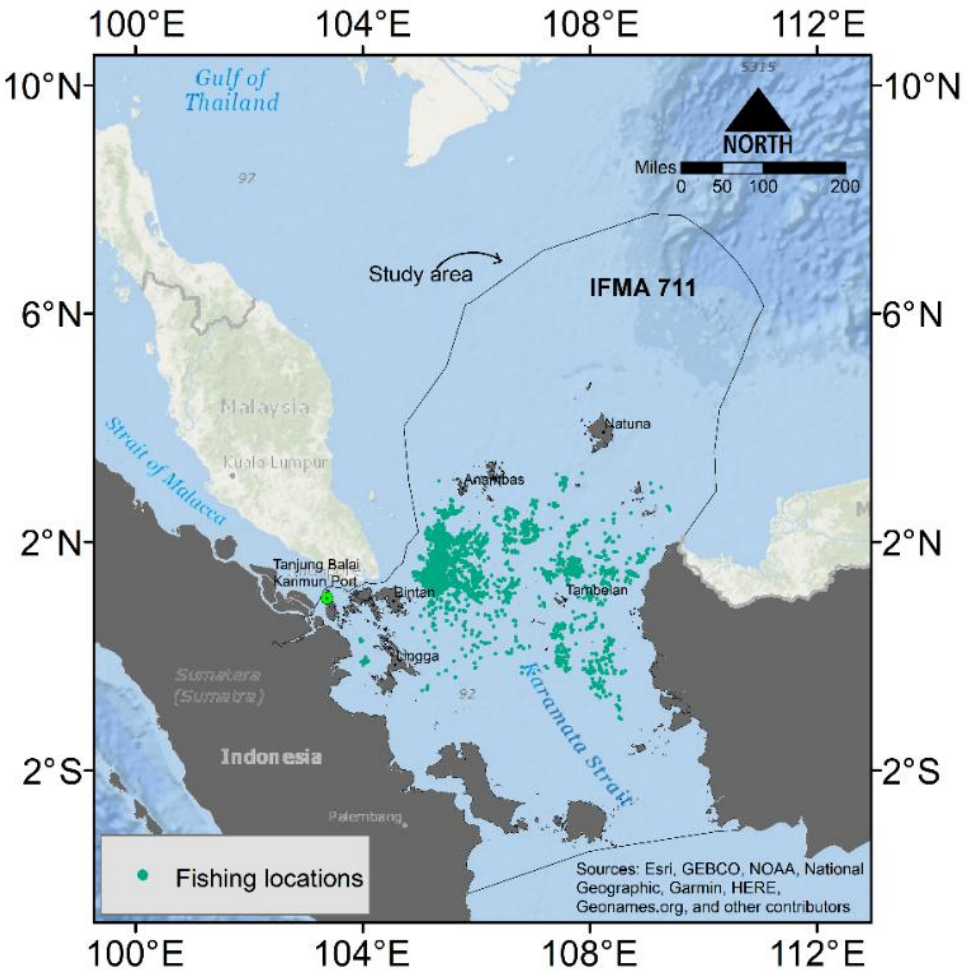

Fig. 1. The map depicts the IFMA 711 as a study area, and the green color represents the vessel locations for catching MS based on filtering VMS data

Table 1. The characteristics of oceanographic data

Data type	Description	Unit	Data source
Sea surface temperature (SST)	Monthly SST on the spatial resolution of 4 km	°C	http://oceancolor.gsfc.nasa.gov
Sea surface chlorophyll-a (CHL)	Monthly CHL on the spatial resolution of 4 km	mg m^{-3}	http://oceancolor.gsfc.nasa.gov
Bathymetry	Elevation data on a 15 arc-second interval grid	m	http://gebco.net

2.3. Environmental data

This study used bathymetry, sea surface temperature, and chlorophyll-a concentration obtained from satellite remote sensing data (Table 1). They are along with

the fishing month and geographic location (latitude, longitude) as predictor variables to identify the variability of the MS catch rate.

2.4. Data preparation and processing

Research data were prepared and processed at the Ocean and Coastal Remote Sensing Laboratory, Center for Coastal Rehabilitation and Disaster Mitigation Studies of Diponegoro University in Semarang, Indonesia. In brief, the first step was determining the fishing effort of cast net vessels from VMS data (Fig. 2). Then, the catch in each fishing location was identified. The yield was compared with the fishing effort to calculate the catch rate over a standardization spatial of 0.25°×0.25° (latitude×longitude). Then, the same action, reprojecting to standard spatial resolution, was applied to satellite remote sensing data. The spatial data were monthly summarized for analysis with GAM. Processing all spatial data used ArcGIS v10.8 **(ESRI, 2011)**. The GAM was built using the MGCV library in R v4.0.0 **(R Core Team, 2020)**. It was practiced to examine the effects of temporal, spatial, and marine environmental factors on the MS catch rate. Finally, the output data from the best model was used to determine productive fishing grounds.

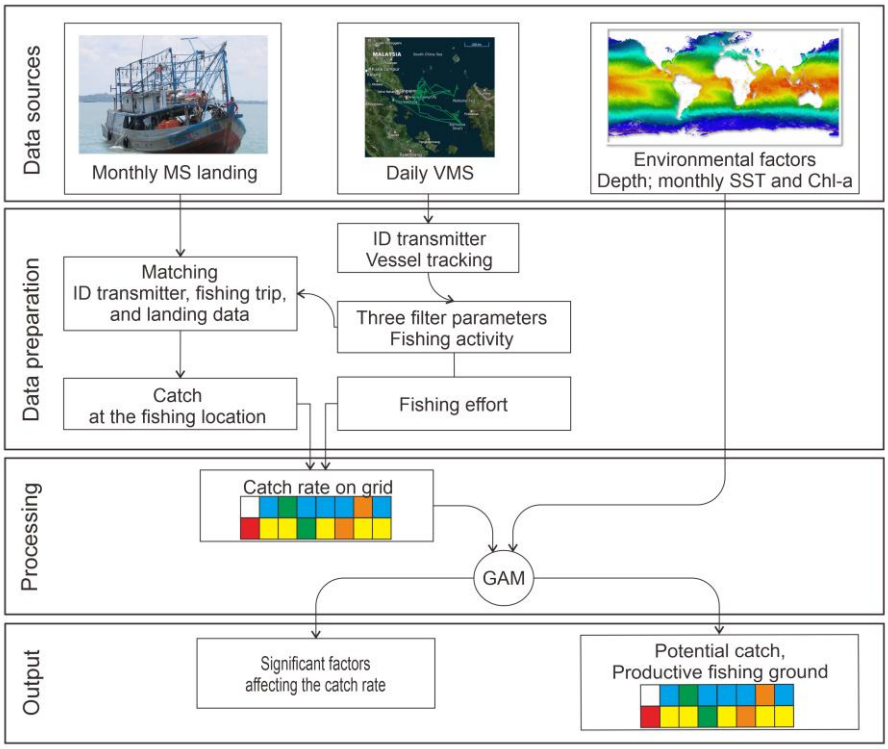

Fig. 2. Review all steps to identify the factors affecting the catch rate and mapping potential catch

2.5. Assumptions in determining fishing activity

VMS data is a daily vessel tracking in the form of point data, with each point (ping) having a time interval ranging from 1 minute to 1 hour. In this study, 1-hour

intervals, the most recent data, were used for sorting and accumulating vessel tracking data. Initially, the daily VMS trajectory did not provide detailed information about vessel activities. As a result, distinguishing between fishing and other vessel activity became necessary. Fishing activity was defined in this study as the time the vessel spends between lowering the anchor to catch squid and raising the anchor to find a new fishing location. Three parameters were used as a filter to detect fishing activity:

2.5.1. Fishing time

The cast net operated at night based on the fishing technique. As a result, the time chosen was from 6 pm to 5 am on the next day, which corresponds to the time zone when the sky is dark, as the first filter to determine fishing activity.

2.5.2. Vessel speed

The vessel speed was commonly used to evaluate fishing activity from VMS data **(Feng *et al.*, 2019; Gerritsen & Lordan, 2011)**. The cast net operation began with dropping the anchor to make the boat more stable, then falling the open net onto a schooling squid. As a result, the fishing effort was calculated based on a speed of 0 (zero) knots caused by a drop in anchor during fishing operations. In this filter, the zero boat speed was neglected due to engine failure.

2.5.3. Fishing area

According to **MMAF (2020)**, the fishing area of cast net vessels operates more than 12 miles from the shoreline. This filter eliminates an unnecessary zero-speed trajectory caused by the vessel's position in port or sheltering on a nearby island during adverse weather conditions.

2.6. Catch rate calculation

The landing data per vessel included records of catches made during a single fishing trip at multiple fishing locations. Consequently, the yield per fishing location had to be recalculated to correspond with the fishing effort at the fishing location. A step to verify fishing activity (from VMS trajectory) and squid landing data was required based on the transmitter ID and fishing hours to measure the number of catches at each fishing location.

The estimation of catch per fishing location was calculated by following the LPUE method **(Russo *et al.*, 2018)**, with modification of the fishing power variable. In this study, the vessel productivity (VP) was used to substitute the fishing power related to vessel size (GT_v). The VP was calculated by dividing the number of fish caught (in tons) per type of fishing gear by the vessel size (in gross tonnage) during one year **(MMAF, 2021)**. Calculating the fishing power (FP) of the vessel (v) using the following formula (Equation 1):

$$FP_v = VP \times GT_v \times 1000/8760 \quad (1)$$

Where, VP for cast net vessel is 0.86 **(MMAF, 2021)**, the multiplier (1000/8760) denotes the conversion of tons per year to kg per hour.

Consequentially, if $F_{l,t,v}$ is the total duration of the fishing activity (in hours) conducted by a vessel (v) during fishing trips occurring on fishing ground (l) during the period (t), and GT is the size of the vessel (v), the fishing effort, FE, is obtained by (Equation 2):

$$FE_v = FP_v \times F_{l,t,v} \quad (2)$$

It also implies that the average of the MS catches at each fishing location (kg), $c_{l,t,v}$, corresponding to the fishing activity (e) of a vessel (v) at time (t) in the fishing ground (l) was acquired by (Equation 3):

$$c_{l,t,v} = \frac{TC_v}{FE_v} \times e_{l,t,v} \quad (3)$$

Where, TC_v is the amount of squid landing by vessel in one fishing trip, corresponding with record landing data.

Following the acquisition of data on fishing activity and catch at each fishing location, the catch rate was examined using a geospatial approach by regarding **Adibi *et al*. (2020)** with modification of the spatial grid. As a fishing grid, a spatial of 0.25°× 0.25° (latitude × longitude) was used. The technique created a raster layer from the value of the catch and fishing activities. Then, the catch rate was calculated by dividing the MS caught (kg) by the number of hours of fishing activity from all vessels on the fishing grid. As a result, the fishing grid's MS catch rate was calculated as follows (Equation 4):

$$CR_{l,t} = \frac{\sum c_{l,t,v}}{\sum e_{l,t,v}} \quad (4)$$

Where, $CR_{l,t}$ is catch rate (kg h^{-1}) at location l at time t.

The catch rate data were overlaid on the fishing grid and summarized monthly. Each fishing grid was used to extract the raster pixel values of the corresponding fishing location. This information was compiled into a single data set that included fishing location and pixel data. This spatial analysis unit is assumed to be the interconnection of the spatial extent scale and the accuracy of squid fishing locations.

2.7. Identifying geographical and oceanographic characteristics in fishing grounds

The general characteristics of the geographical location and oceanographic characteristics of squid fishing activities by cast net vessels in the fishing ground were determined using monthly average data. The formula used in the calculation was:

$$\overline{P}_m = \frac{1}{N} \times \sum_{n=1}^{N} P_{m,n} \quad (5)$$

Where, $\overline{P}_m$ is the average longitude (or latitude or depth or CHL or SST) in the fishing location after data fusion to the fishing grid in month m; N is the number of the fishing grid; $P_{m,n}$ is the value of longitude (or latitude or depth or CHL or SST) in month m and period n.

2.8. GAM analysis

The procedure for GAM fitting in the case of data with catch rate response variables and environmental factor predictors used the Gaussian error distribution with an identity linking function **(Yu *et al.*, 2019; Wang *et al.*, 2020)**. Furthermore, when using GAM, the distribution of catch rate data had to be adjusted from asymmetric to symmetric using logarithmic transformation **(Hoyle *et al.*, 2014)**. The current study allowed these recommendations. Then, the F-test was used to determine whether the predictor variables had a significant effect on the response variable, with a significance level of 1% (P<0.01). A stepwise forward strategy was utilized to choose factors that impact the model for determining the particular expression of GAM. The selection of the best fit model results in the GAM was based on the smallest Akaike's Information Criterion (AIC) for each GAM model formed **(Wood, 2017)**. The model selected for fitting was formulated as follows (Equation 5):

$$\ln CR = s(Month) + s(Long) + s(Lat) + s(Depth) + s(CHL) + s(SST) \quad (6)$$

Where, $\ln CR$ is the logarithmic transformation of the observed catch rate value; s is the spline smoothing function of the variable, and $s(Month)$ represents the effect of the fishing month. Furthermore, $s(Long)$ and $s(Lat)$ are the effects of the longitude and latitude degree of fishing locations, respectively. Finally, $s(Depth)$, $s(CHL)$, and $s(SST)$ are the effect of depth, chlorophyll-a concentration, and sea surface temperature, respectively.

2.9. Model validation and mapping of fishing ground

The accuracy of the best model chosen was evaluated by comparing the observed catch rate with the model output value using mean absolute percentage error (MAPE). This strategy was employed by considering the characteristics of the empirical data, which showed no zero or close to zero value. MAPE has the substantial disadvantage of producing infinite or undefined values for zero or near actual values **(de Myttenaere *et***

***al*., 2016; Kim & Kim, 2016)**. MAPE measures forecasting error concerning the dataset's actual value, which is obtained by dividing the absolute error in each period by the observed values for that period. The average of those fixed percentages of the results was then calculated. It was formulated as follows (Equation 6):

$$MAPE = \frac{1}{N} \times \sum_{i=1}^{N} \left| \frac{y_i - \hat{y}_i}{y_i} \right| \times 100\% \quad (7)$$

Where, N is the number of sample data; y_i represents the observed data in period i, and $\hat{y}_i$ is the predicted data in period i. The MAPE values were interpreted following **Chang *et al*. (2007)** as described in Table (2).

The productive fishing grounds were mapped based on the model output. In raster data, the range of predictor variable values that affect the increase or decrease in catch rate value was grouped as references. These rasters were generated for all months and fishing locations and then analyzed using a raster overlay by additions for suitability modeling. This analysis compiles the rasters into a single data set that is summarized monthly. All monthly rasters were compared and reclassified to obtain high and low-ranking values as a catch potential database. Model performance was assessed by comparing this catch potential with the observed catch rate data set.

Table 2. The interpretation of MAPE

MAPE value	Signification
<10%	Excellent forecasting ability
10–20%	Good forecasting ability
20–50%	Reasonable forecasting ability
>50%	Bad forecasting ability

RESULTS

3.1. Fishing activity, catch, and catch rate

Filtered with the three parameters (fishing time, vessel speed, and fishing area) on VMS data (a total of 418,453 points), only 1.3% identified fishing activity (Fig. 1, green color). In Fig (1), one mark of the fishing location represents a one-hour fishing interval between the 0 (zero) knot speed point and the previous point in the VMS trajectory. From February to October, fishing activities were scattered in the marine waters of Natuna, Anambas, Bintan, Tambelan and Lingga.

The fishing operation of cast nets for 2020 in IFMA 711 occurred from February to November (Table 3). Cast nets departed for fishing locations from February to June, with the highest number of departures in March, 34 units. The number represented more than

half the vessels operated in 2020. Based on the analysis of VMS trajectories, the monthly total fishing activity ranged from 17 to 1,627 hours. A high total number of hours may indicate the number of detected fishing locations. The catch at the fishing location described the average number of catches per haul per hour. In general, the number of catches at the fishing location is proportional to the abundance of squid at the fishing grounds, which is also related to the number of fishing hours. In April, the number of catches at the fishing locations reached the highest value of 357.9 tons, as well as the highest fishing hour value.

In addition, from March to November, cast nets with enough catch gradually returned to the port, with a fishing trip length ranging from 43 to 129 days. In general, the current month's monthly mean of fishing days for vessel arrivals was longer than the previous month. The total monthly landing at the port tended to increase as more vessels arrive to land their catch. The largest catch landing of 457.4 tons occurred in May, with 35 vessels landing. The lowest was 2.4 tons in November, with only one cast net landing. According to data from the day of fishing, the cast nets that landed in May were from vessels departing between February and April. The high number of landings in May appears to be the result of both the large number of vessels landing and the high number of catches per location in April. Overall, the total MS land at the Tanjung Balai Karimun port in 2020 was approximately 1,151.2 tons.

Table 3. Monthly summary of cast net vessel operation analysis data for 2020

Month	Number of vessels depart (units)	Total fishing activity (hours)	Total catch at the fishing location (tons)	Number of vessels arrival (units)	Days of fishing (Mean±SD)	Total landing at the port (tons)
February	13	17	10.3			
March	34	754	172.8	1	43±0	15.6
April	25	1627	357.9	5	49±6	28.5
May	26	1362	304.8	35	66±19	457.4
June	15	459	95.6	19	73±7	254.9
July		331	89.7	16	87±13	135.5
Augustus		352	61.8	22	96±6	180.6
September		286	38.6	8	103±6	42.1
October		84	19.8	6	119±5	34.2
November				1	129±0	2.4

In this study, the catch rate data were overlaid on the fishing grid of 0.25° × 0.25° (latitude × longitude) and summarized monthly. The number of monthly fishing grids varied from 9 to 100, with the highest value in April (Fig. 3a). The number of grids

represents the distribution of fishing locations. The greater the number of grids, the larger the fishing area. The monthly mean of catch rate showed the lowest at 89.43 kg h^{-1} in October and the highest at 337.47 kg h^{-1} in May **(Fig. 3b)**. The standard deviation of the monthly catch rate indicated a value of more than half the mean reflecting a large amount of variation in the data.

The total catch at the fishing location, the number of fishing grids, and total fishing activity were all higher in April than in May, but the mean catch rate was higher in May than in April **(Table 3 & Fig. 3)**. This demonstrates that a high mean catch rate on the grid will not always be linear with a high total catch at a fishing location, depending on the number of fishing grids and total fishing activity.

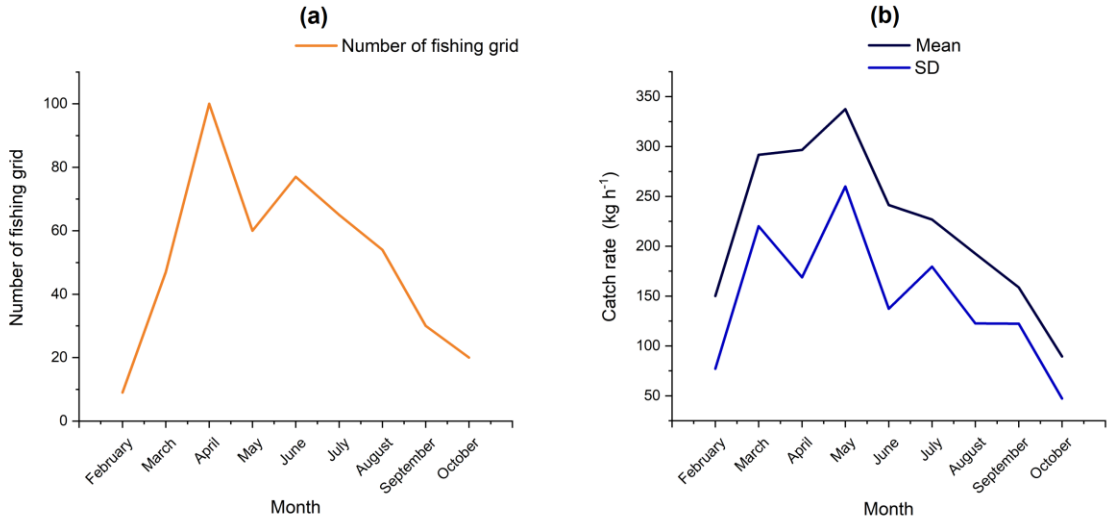

Fig. 3. Monthly variation in the number of fishing grid and catch rate from February to October 2020

3.2. Monthly variation in geographical and oceanographic characteristics in the fishing grounds

The information on longitude, latitude, depth, CHL, and SST demonstrated variations in the fishing grounds. The longitude variability was 104°-109.5° E; the latitude was 1.22° S-3.28° N; the CHL density was 0.09-1.00 mg m^{-3}, and the SST was 27.6-32.2 °C. It used data based on monthly mean values of all fishing grids corresponding to the catch rate to describe the variability of oceanographic parameters.

The fishing ground shifted from low latitudes and longitudes to higher elevations from February to April (Fig. 4). At the same time, the water temperature gradually increased. The density of CHL decreased from February to March, then increased from March to April; whereas, the depth revealed the opposite condition as the CHL parameter. From May to July, the fishing grounds moved to a lower latitude than the previous month, despite the degree of longitude which showed a movement to a lower

area in May and then increased from June to July. The SST conditions remained elevated from May to June, before declining in July. The changes in depth and CHL characteristics were similar to the prior three months.

Furthermore, from August to September, the fishing grounds shifted to areas with lower latitudes but higher longitudes than the previous month. The SST conditions in August and September were similar but lower than in July. The depth of the fishing ground in August and September remained shallower than in the preceding month, with CHL density increasing during July. Finally in October, the fishing grounds shifted to a site with a higher latitude though being a lower longitude than the previous month. Simultaneously, the fishing grounds changed to a deeper location with lower SST and CHL conditions.

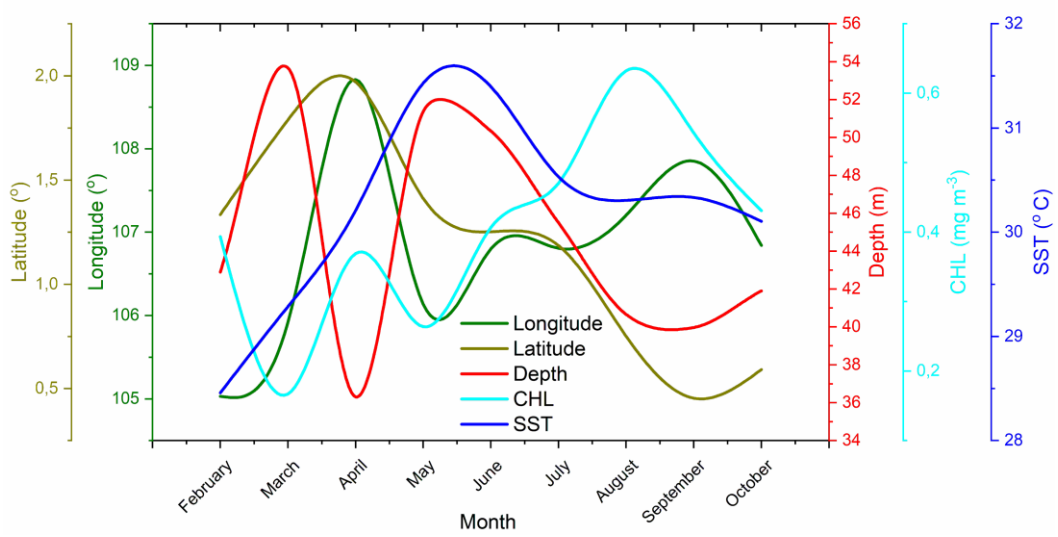

Fig. 4. Monthly variability of longitude, latitude, depth, CHL, and SST variables for MS fishing grounds from February to October 2020

3.3. GAM analysis

The GAM was used to analyze the relationship between catch rate as a response variable and predictor variables including fishing month, longitude and latitude of the fishing location, depth, chlorophyll-a, and sea surface temperature based on grid data. The univariate model was used to analyze the influences of each predictor variable on catch rate and the corresponding fitting degree of the model **(Table 4)**. Each variable has a different impact on the MS catch rate. Variables were selected based on the F-test with a significant level of 1% ($P < 0.01$). All six predictor variables passed the significance test, indicating that each variable was statistically significant in influencing the catch rate, with low deviance explained. It was discovered that the sequence influence of variables was SST < CHL < Long < Depth < Lat < Month based on the deviance of each variable. Month and latitude explain more deviance, with values of 23% and 10.2%, respectively.

Table 4. Test of each predictor variable in GAM.

Variable	df	edf	DE	*F-value*	*p-value*
s(Month)	6.95	4.95	23%	17.62	<2e-16 ***
s(Long)	4.65	6.19	6.23%	2.79	0.00648 **
s(Lat)	8.19	2.65	10.2%	12.12	1.05e-07 ***
s(Depth)	8.39	6.39	7.9%	3.70	0.000461 **
s(CHL)	3.00	1.00	4.69%	18.29	2.45e-05 ***
s(SST)	5.56	3.56	3.45%	2.43	0.0445 *

Significance codes: 0 '***' 0.001 '**' 0.01 '*'

The univariate analysis of general additive modeling revealed that each predictor variable had a low precision. Consequently, multi variables are needed to investigate their effect on MS catch rates. Predictor variables were incrementally entered into GAM and selected using the AIC score **(Table 5)**. It has been shown that as the number of variables increased, the AIC score decreased, and the value of deviance explained in the model increased, indicating an increase in the fit and generalization of the model. The results of GAM fitting showed that the best model for MS included six explanatory variables. The deviance explained by this model was 32.9%, with an AIC score of 606.12. The relationship between the catch rate and each variable in the GAM aided in determining the significance of each variable sequentially **(Table 6)**. According to the F-ratio test, three variables in the best model were significant (P<0.01), consisting of Month, Latitude, and SST, with contribution values of 42.6.2%, 33.6%, and 12.7%, respectively.

Table 5. Test of the combination of predictor variables in GAM.

Variable	df	AIC	DE
s(SST)	5.56	706.03	3.45%
s(SST)+ s(CHL)	6.21	689.63	7.91%
s(SST)+ s(CHL)+ s(Long)	12.75	687.49	13.4%
s(SST)+ s(CHL)+ s(Long)+ (Depth)	17.48	675.05	16.6%
s(SST)+ s(CHL)+ s(Long)+ (Depth)+ s(Lat)	14.37	667.99	16.8%
s(SST)+ s(CHL)+ s(Long)+ (Depth)+ s(Lat)+ s(Month)	23.66	606.12	32.9%

Table 6. Contribution of each predictor variable in the best fit model.

Index	SST	CHL	Long	Depth	Lat	Month
edf	5.186	3.657	1.000	4.927	1.000	5.890
F-value	3.484	1.037	0.385	1.615	9.217	11.700
P-value	0.0021 **	0.4436	0.5355	0.1527	0.0025 **	<2e-16 ***
Contribution	12.7%	3.8%	1.4%	5.9%	33.6%	42.6%

Significance codes: 0 '***' 0.001 '**' 0.01 '*'

Analysis of GAM in the best fit model generates plots of the effect of predictor variables on the response variable (**Fig. 5)**. Shaded areas in the figures describe the

confidence intervals at the 95% level. The tightly defined confidence limits indicate high relevance distribution scales, while the wide confidence limits represent low relevance distribution scales. The effect of predictor variables on MS catch rate revealed that SST increased the rate of catch significantly at 27.6-29.5 ℃ and 31.5-32.2 °C while tending to decrease at temperatures greater than 29.5-31.5 °C **(Fig. 5a)**. The confidence interval dropped between 27.5 and 31 °C and gradually increased between 31 and 32 °C. At a range of 0.1-0.4 mg m^{-3}, the CHL density formed a wavy plot tends to flatten with a decreased confidence interval and gradually increases to more than 0.4-1 mg m^{-3} **(Fig. 5b)**. The rate of catch decreased when the concentration was less than 0.4 mg m^{-3} or greater than 0.6 mg m^{-3} and increased when the attention was between 0.4 and 0.6 mg m^{-3}. The Depth variable positively affected the MS catch rate **(Fig. 5c)**. The more profound the fishing location, the higher the catch rate, with a confidence interval, gradually decreasing to 20-45 m and progressively increasing to 45-80 m. The catch rate increased as the latitude degree increased, indicating a linear positive effect on latitude **(Fig. 5d)**. The confidence interval for the latitude effect decreased gradually from 1° S-1° N before gradually increasing from 1°-3° N. The longitude variable influenced the decrease in catch rate in the fishing area from 104° to 105° E, reducing the confidence interval progressively. The catch rate steadily increased with the significance interval level at more than 105°-109.5° E **(Fig. 5e)**. The fishing month variable had a dome-shaped relationship **(Fig. 5f)**. The catch rate gradually increased from February to May, then declined from June to October.

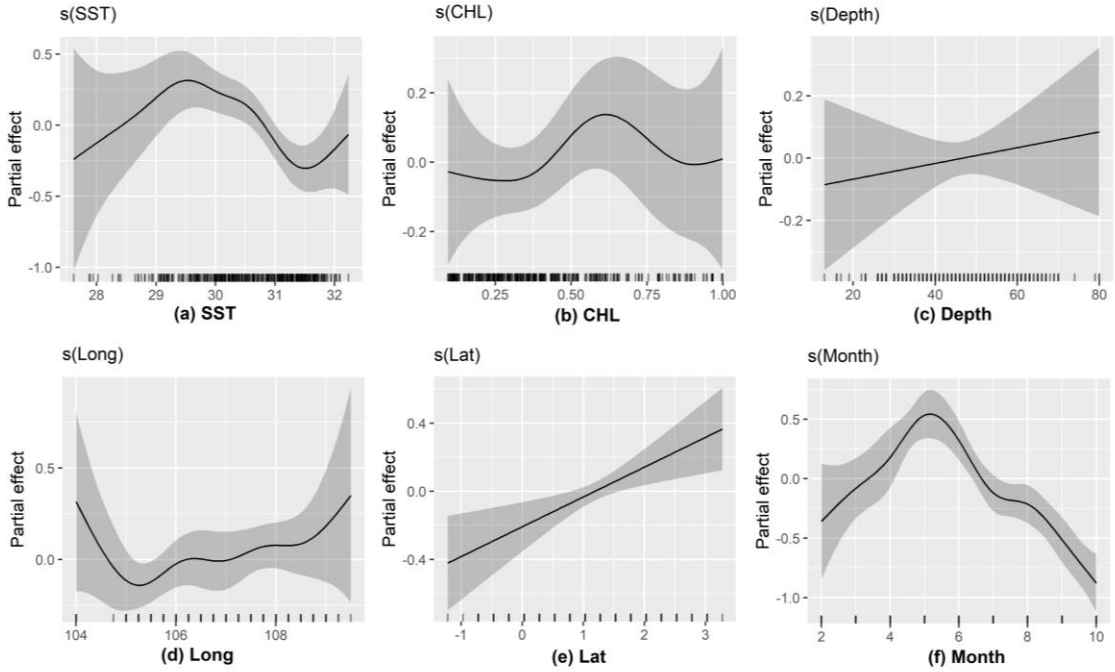

Fig. 5. Effect of predictor variables on catch rate in the best fit model: (a) SST, (b) CHL (c) depth, (d) longitude, (e) latitude, and (f) month of fishing. On the x-axis, rug plots depict the relative density of data points.

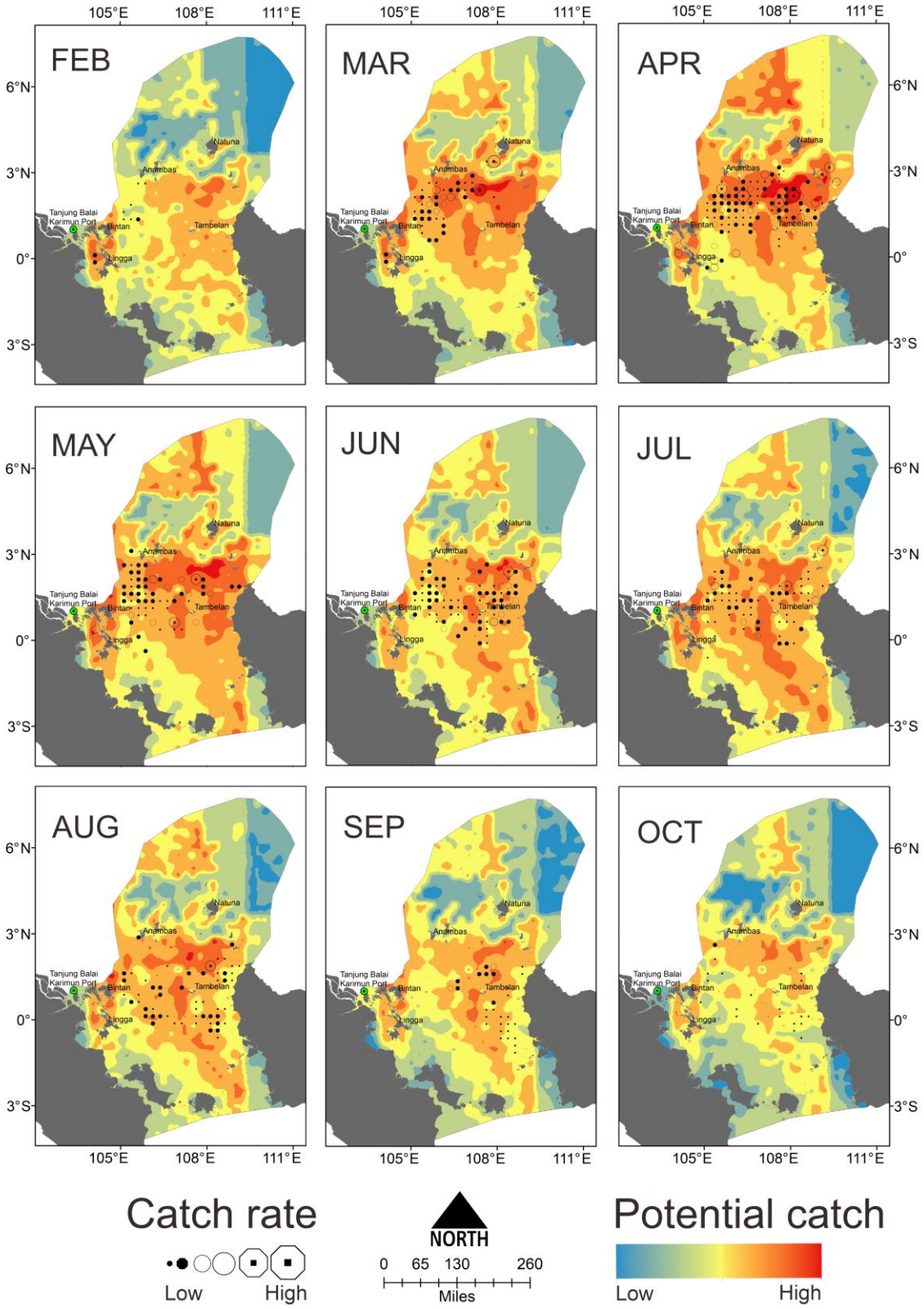

Fig. 6. Monthly raster maps of productive fishing grounds. The circle symbol represents the observed catch rate data, and the color ramp denotes the predicted potential catch.

3.4. Model validation and mapping fishing ground

The accuracy of the best fit model based on MAPE analysis produces an error rate of 7.5%, which means it has an excellent forecasting ability. The data output of the best fit model was used to forecast potential catch in a raster map summarized monthly **(Fig. 6)**. Prediction results are validated by combining them with observed catch rates. Both the catch rate and the catch potential are graded from low to high. The catch rate is represented by a circle, with the larger the circle indicating a higher catch rate. While the catch potential is represented by a color ramp with blue at the lowest and red at the highest part. We discovered that high catch rates were related to high catch predictions. A higher catch potential indicates an area that better fits the range of predictor variable values identified in the model. The availability of data for high catch rates in areas with high catch potential shows the model explains the distribution of fishing ground well. Productive fishing grounds are marked on the prediction map with a red area and a large circle around this one. It was found mainly in the waters between Anambas, Natuna, and Tambelan. This indicates that the waters are the most productive fishing ground.

DISCUSSION

This study demonstrates the use of models to understand factors affecting catch rates and estimate potential catch for determining productive MS fishing grounds. A fishing effort analysis that specifies the time and location of fishing is required to provide the catch rate analysis. It might be the first study to spatially analyze cast net fishing efforts from VMS data in the IFMA 711 part of the Indonesian Sea. Previously, **Marzuki *et al.* (2015)** studied fishing activity from VMS data for the shrimp trawler, purse-seiner, pole-and-liner, and longliner operating in the IFMA 718. The VMS records spatially cast net vessel activities during a fishing trip. As a result, the utility of VMS data can be advanced in squid resource monitoring because the analyses of data offered by this system allow for the mapping and quantitative determination of fishing efforts.

The geographically referenced fishing effort with corresponding catch landings is used to calculate catch rates, which are widely used as indicators of abundance **(Russo *et al*., 2018)**. Therefore, this approach might be a reliable alternative in providing spatial information related to potential catches in the fishing ground. A database was created with MS landing data, VMS-based fishing efforts of cast net vessels, and oceanographic satellite images. It is used to analyze catch rates according to the oceanographic conditions and obtain models that provide more information about the productivity of the fishing grounds. In Addition, we used GAM to assess the effect of the fishing month, geographic fishing location, and oceanographic variables on catch rates.

Few studies have been conducted previously to develop a model for the spatial prediction of squids in other oceanic regions. **Tian *et al.* (2009)** studied *Ommastrephes bartramii* for Chinese Squid-jigging fishery in the Northwest Pacific Ocean to

standardize catch per unit effort using two statistical models, the generalized linear model (GLM) and GAM. They noticed that GAM analysis performs better than GLM analysis to understand abundance variability in time and space. **Yu *et al*. (2019)** studied *Sthenoteuthis oualaniensis* in the north-central South China Sea using GAM to successfully understand the response of squid abundance to marine environment changes. Additionally, according to **Solanki *et al*. (2017)**, the GAM allows any user to identify the fishing grounds corresponding with a range of environmental parameters suitable for squid abundance. Concerning squid abundance prediction, **Denis *et al*. (2002)** explained that the general additive modeling, although inaccurate in predicting squid abundance in small geometric areas, can indicate where productive fishing grounds are expected.

In the present study, squid fishers start fishing operations in February **(Table 3)**. This month is the end of the wet season in Indonesia, where high rainfall in previous months encourages an increase in nutrients from river runoff and causes higher chlorophyll-a concentrations in coastal areas. Coastal upwelling may also affect the nutrient increase. Nutrients originating from coastal upwelling off northwest Borneo in the South China Sea were carried by currents to IFMA 711, formed in December, matured in January, and decayed in February **(Yan *et al*., 2015)**. Then, the transition to the dry season caused a rise in SST from March to May. The growing concentration of chlorophyll allowed by the increase in temperature and nutrients on the coast caused waters to have high productivity and be food-rich, impacting the increase in the MS abundance. The GAM analysis findings indicate that the highest catch rate occurred in May when the mean SST in the fishing grounds gradually increased over three months **(Fig. 4)**. These results corroborate previous studies by **Suwarso *et al*. (2019)** in the Karimata strait, part of IFMA 711. They found a higher MS abundance in April-May led to a high catch rate.

In GAM analysis, we employed three oceanographic data: bathymetry, chlorophyll-a, and sea surface temperature. In the univariate model, Depth was the oceanographic parameter with the most influence on the MS catch rate compared to CHL and SST. The MS exhibited significant vertical diel migration, beginning in deep waters during the day and moving up to surface waters at night (0 to 200 m) **(Jereb and Roper, 2010)**. Sea depth was also related to the squid migration, spawning ground in coastal waters, and feeding ground farther offshore **(Arkhipkin *et al*., 2015)**. The Depth variable may significantly affect the catch rate in the univariate test. However, in the best model fit of the multivariate test, the Depth variable does not firmly explain the response variable. **Denis *et al*. (2002)** documented that bathymetry does not play a significant role in the overall pattern of squid abundance. Still, it could contribute to inter-seasonal differences when combined with climatic variables and life-cycle-sensitive stages over time.

In the best model fit, three significant variables affected the MS catch rate: month, degree of latitude, and sea surface temperature. Compared with previous relevant studies, it was known that certain months affect the life stages of squid and their growth rate, resulting in changes in monthly biomass stocks. In January, female and male squid mature faster in North Queensland waters **(Jackson *et al.*, 2012)**. March and April are spawning months in the South China Sea when more male and female squid swarm **(Wang *et al.*, 2010)**. Squids are abundant in the Pearl River Estuary from December to February **(Wang *et al.*, 2021)**. Several researchers have reported the effect of a specific range degree of latitude on a high abundance of squid. **Chang *et al.* (2016)** found that the *Illex argentinus* abundant in the Southwest Atlantic was elevated at 40°–50° S. Whereas, **Pilar-Fonseca *et al.* (2013)** reported that *Loligo vulgaris* off the Portuguese coast showed a high density at 36.5–41.5° N. The temperature variations substantially impacted squid prevalence and distribution shifts **(Agnew *et al.*, 2002; Chasco *et al.*, 2022)**. Temperature dynamics on an annual scale were linked to trends in squid landings **(Robin and Denis, 1999)** and positively increased squid catch rates in warmer water **(Wang *et al.*, 2021)**. The concentration of squid is abundant at different temperature ranges depending on the species and fishing location. **Tian *et al.* (2009)** found the catch rate of *Ommastrephes bartramii* in the Northwest Pacific Ocean tended to rise in the temperature range of 14–21 °C. While in the South China Sea, the catch rate of squid (*Sthenoteuthis oualaniensis*) increases when the temperature is 24–28 °C **(Yu *et al.*, 2019)**.

The MAPE was used to assess the accuracy of the best fit model. This method was appropriate for determining the accuracy of a prediction when the predicted sample was acknowledged to remain significantly above zero **(de Myttenaere *et al.*, 2016)**. Furthermore, **Prayudani *et al.* (2019)** found that it was advantageous when the quantity of predictive factors is critical in determining prediction performance. An accuracy test based on a percentage of error was scale-independent. It was commonly used to compare estimated performance across diverse data series **(Hyndman and Koehler, 2006)**.

The output data from the best fit model was used to forecast the potential of MS catch as an indicator to determine productive fishing grounds. The prediction results were represented on a map, indicating which locations were low or high in MS abundance. The availability of information concerning productive fishing grounds allows for greater flexibility in management strategies. For example, vessels may be directed to the most valuable areas with the highest potential catch, preventing fishing in low-value areas to allow resources to reach a state of readiness for capture.

Nonetheless, the results of this study should be interpreted with caution, and certain limitations should be considered. In this study, MS catches were calculated on average from all fishing locations in all months in one fishing trip. This approach can cause catch rate prediction bias in the model analysis even though the accuracy is high.

Therefore, the catch per fishing location with geographic coordinates from observer or master fishing records can be used to overcome data limitations.

CONCLUSION

Information on productive fishing grounds is useful in supporting marine spatial planning and management of squid resources. In our opinion, the GAM approach, when combined with geospatial techniques, is capable of describing the factors that influence catch rates and mapping productive fishing grounds. The combination of VMS, landing, and satellite remote sensing data has the potential to be the most practical and cost-effective method of analyzing the dynamics of fishing grounds at multiple time and space scales. This research adds value to VMS data for identifying fishing locations and aids in determining the oceanographic conditions of fishing areas.

The study results indicated the need for a strategy to be efficient in fishing efforts because most of the operating time of vessel was spent on activities other than fishing. We found three major parameters influencing the catch rate of miter squid: fishing month, latitude degree of fishing grounds, and sea surface temperature. These three factors have the possibility to serve as guidelines in finding miter squid fishing grounds to increase the efficiency of fishing efforts. The most productive fishing grounds were identified in the waters between Anambas, Natuna, and Tambelan. These findings can support marine spatial planning and squid resource management in IFMA 711.

REFERENCES

Adibi, P.; Pranovi, F.; Raffaetà, A.; Russo, E.; Silvestri, C.; Simeoni, M.; Soares, A. and Matwin, S. (2020). Predicting Fishing Effort and Catch Using Semantic Trajectories and Machine Learning. Lecture Notes in Computer Science (Including Subseries Lecture Notes in Artificial Intelligence and Lecture Notes in Bioinformatics), 11889 LNAI, pp. 83–99. DOI: 10.1007/978-3-030-38081-6_7

Agnew, D.; Beddington, J. and Hill, S. (2002). The potential use of environmental information to manage squid stocks. Can. J. Fish. Aquat. Sci., 59(12): 1851–1857. DOI: 10.1139/f02-150

Alabia, I. D.; Saitoh, S. I.; Mugo, R.; Igarashi, H.; Ishikawa, Y.; Usui, N.; Kamachi, M.; Awaji, T. and Seito, M. (2015). Identifying Pelagic Habitat Hotspots of Neon Flying Squid in the Temperate Waters of the Central North Pacific. PLOS ONE, 10(11): 1–20. DOI: 10.1371/journal.pone.0142885

Arkhipkin, A.I.; Rodhouse, P.G.K.; Pierce, G.J.; Sakai, M.; Allcock, L.; Arguelles, J.; Bower, J.R.; Ceriola, L.; Chen, C.; Chen, X.; Diaz-santana, M.; Downey, N.; González, A.F.; Amores, J.G.; Green, C.P.; Guerra, A.; Hendrickson, L.C.; Ibáñez, C.; Ito, K. and Granados-amores, J. (2015). World Squid

Fisheries. Reviews in Fisheries Science and Aquaculture, 23(2): 92–252. DOI: 10.1080/23308249.2015.1026226

Chang, K.Y.; Chen C.S.; Chiu, T.Y.; Huang, W.B. and Chiu, T.S. (2016). Argentine Shortfin Squid (*Illex argentinus*) Stock Assessment in the Southwest Atlantic Using Geostatistical Techniques. Terr. Atmos. Ocean. Sci., 27: 281–292. DOI: 10.3319/TAO.2015.11.05.01(Oc)

Chang, P.C.; Wang, Y.W. and Liu, C.H. (2007). The development of a weighted evolving fuzzy neural network for PCB sales forecasting. Expert Systems with Applications, 32(1): 86–96. DOI: 10.1016/j.eswa.2005.11.021

Chasco, B.E.; Hunsicker, M.E.; Jacobson, K.C.; Welch, O.T.; Morgan, C.A.; Muhling, B.A. and Harding, J.A. (2022). Evidence of Temperature-Driven Shifts in Market Squid *Doryteuthis opalescens* Densities and Distribution in the California Current Ecosystem. Marine and Coastal Fisheries, 14: 1–13. DOI: 10.1002/mcf2.10190

Crespo-Neto, O.; Díaz-Delgado, E.; Acosta-Pachón, T.A. and Martínez-Rincón, R.O. (2021). Spatial segregation by size of billfishes bycaught by the tuna purse-seine fishery in the Eastern Pacific Ocean. Fisheries Research, 241: 1–11. DOI: 10.1016/j.fishres.2021.106001

de Myttenaere, A.; Golden, B.; Le Grand, B. and Rossi, F. (2016). Mean Absolute Percentage Error for regression models. Neurocomputing, 192: 38–48. DOI: 10.1016/j.neucom.2015.12.114

Denis, V.; Lejeune, J. and Robin, J.P. (2002). Spatio-temporal analysis of commercial trawler data using General Additive models: Patterns of Loliginid squid abundance in the north-east Atlantic. ICES J. Mar. Sci., 59(3): 633–648. DOI: 10.1006/jmsc.2001.1178

ESRI. (2011). ArcGIS Desktop: Release 10. CA: Environmental Systems Research Institute, Redlands.

Feng, Y.; Zhao, X.; Han, M.; Sun, T. and Li, C. (2019). The study of identification of fishing vessel behavior based on VMS data. In Proceedings of the 3rd International Conference on Telecommunications and Communication Engineering (ICTCE '19), pp. 63–68. DOI: 10.1145/3369555.3369574

Fauziyah; Purwiyanto, A.I.S.; Agustriani, F. and Putri, W.A.E. (2020). Growth aspect of squid (*Loligo chinensis*) from the Banyuasin Coastal Waters, South Sumatra, Indonesia. Ecologica Montenegrina, 27: 1–10. DOI: 10.37828/em.2020.27.1

Gerritsen, H. and Lordan, C. (2011). Integrating vessel monitoring systems (VMS) data with daily catch data from logbooks to explore the spatial distribution of catch and effort at high resolution. ICES J. Mar. Sci., 68(1): 245–252. DOI: 10.1093/icesjms/fsq137

Hastie, T. and Tibshirani, R. (1986). Generalized Additive Models. Statistical Science, 1(3): 297–310. DOI: 10.1214/ss/1177013604

Hyndman, R.J. and Koehler, A.B. (2006). Another look at measures of forecast accuracy. International Journal of Forecasting, 22(4): 679–688. DOI: 10.1016/j.ijforecast.2006.03.001

Hoyle, S.D.; Langley, A.D. and Campbell, R.A. (2014). Recommended approaches for standardizing CPUE data from pelagic fisheries. WCPFC-SC10–2014/SA-IP-10. Western and Central Pacific Fisheries Commission. DOI: 10.13140/2.1.4433.2164

Islam, R.; Pradit, S.; Hajisamae, S.; Paul, M.; Naim, J. and Fazrul, H. (2017). Abundance and distribution pattern of two common Loliginid squids, *Uroteuthis (Photololigo) chinensis* (Gray 1849) and *Uroteuthis (Photololigo) duvaucelii* (d'Orbigny 1835), in the Gulf of Thailand. Asian Fisheries Science, 30: 262–273. DOI: 10.33997/j.afs.2017.30.4.004

Jackson, J.B.C.; Kirby, M.X.; Berger, W.H.; Bjorndal, K.A.; Botsford, L.W.; Bourque, B.J.; Bradbury, R.H.; Cooke, R.; Erlandson, J.; Estes, J.A.; Hughes, T.P.; Kidwell, S.; Lange, C.B.; Lenihan, H.S.; Pandolfi, J.M.; Peterson, C.H.; Steneck, R.S.; Tegner, M.J. and Warner, R.R. (2012). Historical Overfishing and the Recent Collapse of Coastal Ecosystems. Science, 293(5530): 629–637. DOI: 10.1126/science.1059199

Jereb, P. and Roper, C.F.E. (2010). Cephalopods of the world. An Annotated and Illustrated catalogue of Cephalopod species known to date. Vol. 2. Myopsid and Oegopsid squids. FAO Species Catalogue for Fishery Purposes, 2(4). https://www.fao.org/publications/card/en/c/42d0f8a9-1696-5dcb-a323-e8303399a472

Kim, S. and Kim, H. (2016). A new metric of absolute percentage error for intermittent demand forecasts. International Journal of Forecasting, 32(3): 669–679. DOI: 10.1016/j.ijforecast.2015.12.003

Lan, K.W.; Shimada, T.; Lee, M.A.; Su, N.J. and Chang, Y. (2017). Using Remote-Sensing Environmental and Fishery Data to Map Potential Yellowfin Tuna Habitats in the Tropical Pacific Ocean. Remote Sensing, 9(5): 1–14. DOI: 10.3390/rs9050444

Maina, I.; Kavadas, S.; Katsanevakis, S.; Somarakis, S.; Tserpes, G. and Georgakarakos, S. (2016). A methodological approach to identify fishing grounds: A case study on Greek trawlers. Fisheries Research, 183: 326–339. DOI: 10.1016/j.fishres.2016.06.021

Marzuki, M.I.; Garello, R.; Fablet, R.; Kerbaol, V. and Gaspar, P. (2015). Fishing gear recognition from VMS data to identify illegal fishing activities in Indonesia. In OCEANS 2015-Genova: MTS/IEEE international conference, pp. 1–5. DOI: 10.1109/OCEANS-Genova.2015.7271551

MMAF. (2014). Regulation of the Minister of Maritime Affairs and Fisheries of the Republic of Indonesia Number 18/Permen-Kp/2014 concerning the State Fisheries Management Area of the Republic of Indonesia. Ministry of Marine Affairs and Fisheries Republic of Indonesia. http://jdih.kkp.go.id/peraturan/18-permen-kp-2014-ttg-wilayah-pengelolaan-perikanan-negara-republik-indonesia.pdf

MMAF. (2020). Regulation of the Minister of Maritime Affairs and Fisheries Number 59/PERMEN-KP/2020 concerning Fishing Lanes and Fishing Gear in the Fisheries Management Area of the Republic of Indonesia and the High Seas. Ministry of Marine Affairs and Fisheries Republic of Indonesia. http://jdih.kkp.go.id/peraturan/7e7b0-59-permen-kp-2020.pdf

MMAF. (2021). Decree of the Minister of Maritime Affairs and Fisheries Republic of Indonesia Number 98 of 2021 concerning Productivity of Fishing Vessels. Ministry of Marine Affairs and Fisheries Republic of Indonesia. http://jdih.kkp.go.id/peraturan/199b5-2021kepmen-kp98.pdf

Mugo, R.; Saitoh, S.I.; Nihira, A. and Kuroyama, T. (2010). Habitat characteristics of skipjack tuna (*Katsuwonus pelamis*) in the western North Pacific: a remote sensing perspective. Fisheries Oceanography, 19(5): 382–396. DOI: 10.1111/j.1365-2419.2010.00552.x

Naimullah, M.; Lan, K.W.; Liao, C.H.; Hsiao, P.Y.; Liang, Y.R. and Chiu, T.C. (2020). Association of Environmental Factors in the Taiwan Strait with Distributions and Habitat Characteristics of Three Swimming Crabs. Remote Sensing, 12(14): 1–17. DOI :10.3390/rs12142231

Nurdin, S.; Mustapha, M.A.; Lihan, T. and Zainuddin, M. (2017). Applicability of remote sensing oceanographic data in the detection of potential fishing grounds of *Rastrelliger kanagurta* in the archipelagic waters of Spermonde, Indonesia. Fisheries Research, 196: 1–12. DOI: 10.1016/j.fishres.2017.07.029

Pilar-Fonseca, T.; Pereira, J.; Campos, A.; Moreno, A.; Fonseca, P. and Afonso-Dias, M. (2013). VMS-based fishing effort and population demographics for the European squid (*Loligo vulgaris*) off the Portuguese coast. Hydrobiologia, 725(1): 137–144. DOI: 10.1007/s10750-013-1736-x

Prayudani, S.; Hizriadi, A.; Lase, Y.Y.; Fatmi, Y. and Al-Khowarizmi. (2019). Analysis Accuracy Of Forecasting Measurement Technique On Random K-Nearest Neighbor (RKNN) Using MAPE And MSE. J. Phys. Conf. Ser., 1361: 1–8. DOI: 10.1088/1742-6596/1361/1/012089

R Core Team. (2020). R: A language and environment for statistical computing. Vienna, Austria: R Foundation for Statistical Computing. http://www.r- project.org

Rodhouse, P.G. (2001). Managing and forecasting squid fisheries in variable environments. Fisheries Research, 54(1): 3–8.

Robin, J.P. and Denis, V. (1999). Squid stock fluctuations and water temperature: temporal analysis of English Channel Loliginidae. Journal of Applied Ecology, 36(1): 101–110. DOI: 10.1046/j.1365-2664.1999.00384.x

Russo, T.; Morello, E.B.; Parisi, A.; Scarcella, G.; Angelini, S.; Labanchi, L.; Martinelli, M.; D'Andrea, L.; Santojanni, A.; Arneri, E. and Cataudella, S. (2018). A model combining landings and VMS data to estimate landings by fishing ground and harbor. Fisheries Research, 199: 218–230. DOI: 10.1016/j.fishres.2017.11.002

SFP. (2022). Squid: 2021 Sector sustainability update. Sustainable Fisheries Partnership (SFP). https://heyzine.com/flip-book/c8d431ad47.html

Solanki, H. U.; Bhatpuria, D. and Chauhan, P. (2017). Applications of generalized additive model (GAM) to satellite-derived variables and fishery data for prediction of fishery resources distributions in the Arabian Sea. Geocarto International, 32(1): 30–43. DOI: 10.1080/10106049.2015.1120357

Suryanto; Oktaviani, D.; Nugroho, D. and Anggawangsa, R.F. (2021). Fleet diversity of squid fisheries in Indonesia Fisheries Management Area – 711. IOP Conf. Ser. Earth Environ. Sci., 800: 1–9. DOI: 10.1088/1755-1315/800/1/012007

Suwarso, S.; Zamroni, A. and Fauzi, M. (2019). Distribution–Abundance and Catch of the Squids in the Southern Part of Sunda Shelf: Based on the Squids Fisheries Landed in Muara Angke and Kejawanan. Jurnal Penelitian Perikanan Indonesia, 25(4): 225–239. DOI: 10.15578/jppi.25.4.2019.225-239 [Indonesian]

Tian, S.; Chen, X.; Chen, Y.; Xu, L. and Dai, X. (2009). Standardizing CPUE of *Ommastrephes bartramii* for Chinese squid-jigging fishery in Northwest Pacific Ocean. Chinese Journal of Oceanology and Limnology, 27(4): 729–739. DOI: 10.1007/s00343-009-9199-7

Valavanis, V.D.; Pierce, G.J.; Zuur, A.F.; Palialexis, A.; Saveliev, A.; Katara, I. and Wang, J. (2008). Modelling of essential fish habitat based on remote sensing, spatial analysis and GIS. Hydrobiologia, 612(1): 5–20. DOI: 10.1007/s10750-008-9493-y

Wang, D.; Yao, L.; Yu, J. and Chen, P. (2021). The Role of Environmental Factors on the Fishery Catch of the Squid *Uroteuthis chinensis* in the Pearl River Estuary, China. J. Mar. Sci. Eng., 9(2): 1–15. DOI: 10.3390/jmse9020131

Wang, K.; Lee, K. and Liao, C. (2010). Age, growth and maturation of swordtip squid (*Photololigo edulis*) in the Southern East China Sea. Journal of Marine Science and Technology, 18(1): 99–105. DOI: 10.51400/2709-6998.1870

Wang, X.; He, Y.; Du, F.; Liu, M.; Bei, W.; Cai, Y. and Qiu, Y. (2021). Using LBB Tools to Assess Miter Squid Stock in the Northeastern South China Sea. Front. Mar. Sci., 7: 1–8. DOI: 10.3389/fmars.2020.518627

Wang, Y.; Yao, L.; Chen, P.; Yu, J. and Wu, Q. (2020). Environmental Influence on the Spatiotemporal Variability of Fishing Grounds in the Beibu Gulf, South China Sea. J. Mar. Sci. Eng., 8(12): 1–12. DOI: 10.3390/jmse8120957

Wood, S.N. (2017). Generalized Additive Models: An Introduction with R (2nd ed.). Chapman and Hall/CRC. DOI: 10.1201/9781315370279

Yan, Y.; Ling, Z. and Chen, C. (2015). Winter coastal upwelling off northwest Borneo in the South China Sea. Acta Oceanologica Sinica, 34(1): 3–10. DOI: 10.1007/s13131-015-0590-2

Yu, J.; Hu, Q.; Tang, D.; Zhao, H. and Chen, P. (2019). Response of *Sthenoteuthis oualaniensis* to marine environmental changes in the north-central South China Sea based on satellite and *in situ* observations. PLOS ONE, 14(1): 1–16. DOI: 10.1371/journal.pone.0211474